

Data Augmentation for Seizure Prediction with Generative Diffusion Model

Kai Shu, Yuchang Zhao, Le Wu, *Member, IEEE*, Aiping Liu, *Member, IEEE*, Ruobing Qian, and Xun Chen, *Senior Member, IEEE*

Abstract—Objective: Electroencephalogram(EEG)-based seizure prediction is of great importance to improve the life of patients with drug resistant seizures. The focal point of seizure prediction is to distinguish preictal states from interictal ones. With the rapid development of machine learning, seizure prediction methods have achieved significant progress. However, the severe imbalance problem between preictal and interictal data still poses a great challenge to seizure prediction, restricting the performance of classifiers. Data augmentation is an intuitive way to solve this problem. Existing data augmentation methods generate samples by overlapping or recombining preictal data for each seizure. The distribution of generated samples is limited by original data, because such transformations cannot fully explore the distribution of feature space and offer new information. As the epileptic EEG representation varies among seizures, these generated samples cannot provide enough diversity to achieve high performance on a new seizure. As a consequence, we propose a novel data augmentation method with diffusion model called DiffEEG.

Methods: Diffusion models are a class of generative models that consist of two processes, namely the diffusion process and the denoised process. Specifically, in the diffusion process, the model adds noise with different scales to the input EEG sample step by step and converts the noisy sample into output random noise, exploring the distribution of data by minimizing the loss between the output and the noise added. In the denoised process, the model with learned parameters samples the synthetic data by removing the noise gradually, diffusing the data distribution to outward areas and narrowing the distance between different clusters.

Results: We compared DiffEEG with traditional downsampling, sliding window and recombination methods, and then integrated them into three representative classification frameworks(MLP, CNN, Transformer) as backbones. The experiments indicate that DiffEEG could further improve the prediction performance and shows significant superiority to existing data augmentation methods.

Conclusion: This paper proposes a novel and effective method to solve the problem of imbalanced data by using the diffusion model, and demonstrates the effectiveness and generality of our method.

Index Terms—Seizure prediction, deep learning, diffusion model, data augmentation.

Kai Shu, Le Wu, Aiping Liu are with the School of Information Science and Technology, University of Science and Technology of China, Hefei 230027, China.

Yuchang Zhao is with the Department of Biomedical Engineering, Hefei University of Technology, Hefei 230009, China.

Ruobing Qian is with the Department of Neurosurgery, The First Affiliated Hospital of USTC, Division of Life Sciences and Medicine, University of Science and Technology of China, Hefei 230001, China.

Xun Chen is with the Department of Neurosurgery, The First Affiliated Hospital of USTC, Division of Life Sciences and Medicine, University of Science and Technology of China, Hefei 230001, China, and also with the Department of Electronic Engineering and Information Science, University of Science and Technology of China, Hefei 230001, China (e-mail: xunchen@ustc.edu.cn).

I. INTRODUCTION

EPILEPSY is caused by abnormal discharge of brain neurons and is one of the most common neurological disease in the world [1]. According to the World Health Organization (WHO), there are about 70 million people suffered from epilepsy. With the development of modern medical science, 70% of the patients can become seizure-free with appropriate treatment. However, there are still 30% of the patients cannot be controlled by drugs [2]. Therefore, seizure prediction has great value for them. A precise prediction can let patients get timely protection, improving the quality of their lives by reducing their mental stress.

Electroencephalography (EEG) is an efficient technique to record electrical activity of the brain [3]. EEG signals can be divided into three types based on the position where the signals are collected. There is non-invasive scalp electroencephalography (sEEG) with electrodes attached to the subject's scalp, semi-invasive electrocorticogram (ECoG) with electrodes placed between the cerebral cortex and the dura mater, and invasive electroencephalography (iEEG) with implanted electrodes to record the brain's electrical activity [3]. EEG is widely used to diagnose epilepsy in clinical [4] [5]. Over the last few years, studies have shown that EEG signals can help predict the upcoming seizures [6] [7]. In practice, physicians have divided the epilepsy EEG recordings into four states: preictal(period before the onset of seizures), ictal(the duration of seizures), postictal(period that follows the ictal state) and interictal states(interval between seizures) [8]. According to the definitions above, seizure prediction is transferred to a binary classification problem which distinguishes preictal states from interictal ones. In this way, a variety of methods have been proposed to achieve the prediction.

In the traditional machine learning methods, many kinds of manually extracted features have been used to predict seizures, including spatial domain [9], time domain [10], frequency domain [11] [12], and time-frequency domain features [13]. After feature extraction, a classifier is used to do the classification by these features [14]. For instance, Chisci et al. utilized the autoregressive coefficient as features, and a support vector machine (SVM) as classifier [15]. However, extracting features manually needs massive expert experience. In addition, these methods usually exhibit unsatisfactory performance when applied to new patients as features vary greatly among different subjects [16] [17]. Consequently, deep learning(DL) methods have gained growing attention within the last few years, where representative features can be extracted automatically

instead of manually [18] [19]. Li et al. proposed an end-to-end network based on multi-layer perceptrons(MLPs) [20]. The method contains a denoising-weighted block that removes artifacts and assigns weights to each EEG channel, followed by a MLPs block that extracts spatial and temporal features. Gao et al. employed a multi-scale convolutional neural network(CNN) by using the dilated convolutions and adopted an attention-based feature fusion strategy to eliminate redundancy [21]. In another work, Gao et al. proposed a general sample-weighted framework to optimize the sample weights of training sets with genetic algorithm. The contrast experiments is then conducted on SVM, CNN and Transformer with and without the sample weighted to evaluate the effectiveness [22].

All DL algorithms require an extensive amount of labeled data to achieve good performance. However, the scarcity of seizure onsets leads to significant insufficiency of the preictal data for a specific patient [23] [24]. Thus, the composition of dataset is seriously imbalanced with a preponderance of interictal samples, which may lead to overfitting during the training of models [25].

To solve the problem of imbalanced data, a diversity of methods have been taken. Khan et al. down-sampled the interictal data by randomly picking the samples from the data [26]. However, downsampling discards too many interictal samples, which may lead to the loss of useful information. Moreover, deep learning methods usually need a great deal of data to converge to the best performance. After downsampling, the preictal and interictal samples are too small to train the complicated models. Therefore, some researchers proposed data augmentation methods [27] [28]. Data augmentation is the process that generates new samples to augment a small or imbalanced dataset. Troung et al. generated more preictal segments by using an overlapping technique which slid a 30-s window along the EEG signal [29]. Zhang et al. came up with an idea of recombination. For each seizure, they split every training EEG sample into three segments, and then generated new artificial as a concatenation of randomly selected segments [30]. Although those traditional data augmentation methods can increase the number of preictal samples, they are just simple transformations of the existing data with redundant instead of new information. Containing too many repetitive parts, the distribution of generated samples is limited by original data [31]. Due to the nonstationary dynamics in the brain, the epileptic EEG-based representation varies over time [32] and an upcoming seizure may have representation biased from the previous ones. The simple transformations of existing samples can hardly expand the data distribution and cover the variable representation. With the advance of generative model, more and more researchers utilized the generative model to solve the imbalanced data. Rasheed et al. used a generative adversarial network (GAN) to generate synthetic EEG data and evaluated the performance of generated data by a validation method [33]. However, the training process of GAN is difficult. Once the design is improper, the gradient may disappear or explode, resulting in unstable generation quality. In addition, the model may fall into local minimum during training and can only generate samples similar to a limited number of initial data, which is called the mode collapse problem and leads to

the lack of generation diversity [34].

Recently, diffusion models have been widely used in various fields such as computer vision and natural language processing [35] [36]. Diffusion models are a class of promising generative models, which regard the data as a step-by-step diffusion of a series of random noises. They use a Markov chain to gradually add Gaussian noise to data, getting the posterior distribution probability and learning the reverse denoised process. Thus they could synthesise new samples from random noise with the learned distribution of original data [37]. One important use of diffusion model is data augmentation due to its strong generation ability [38] [39] [40]. For example, Chambon et al. utilized a pre-trained latent diffusion model to generate high-fidelity, diverse synthetic chest x-rays(CXR) and measured a 5% improvement of a classifier trained jointly on synthetic and real images [41]. In this paper, we proposed a diffusion-based model named DiffEEG. In specific, DiffEEG consists of two opposite processes, namely the forward/diffusion process and the reverse/denoised process. In the diffusion process, noise with different scales is added to the EEG sample step by step. For each step, the diffusion network converts the noisy sample into random noise conditioned on the initial STFT spectrogram to provide the guiding time-frequency features. By minimizing the loss between the output of the network and the noise added, the feature distribution of preictal data could be fully explored. In the denoised process, based on the learned conditional probability distribution, the synthetic data can be sampled from random noise by gradually removing the noise with different scales, thus diffusing the data distribution to outward area and narrowing the distance between different clusters [42]. The distribution illustration of downsampling, sliding windows, recombination and DiffEEG is presented in Fig. 1.

We train DiffEEG with the patient's preictal EEG signals so that our model can generate synthetic preictal data until we have an equal number of samples per class. The samples are then given to a classifier to conduct seizure prediction task. We used three representative network frameworks(MLP, CNN, Transformer) as classifiers on the CHB-MIT and Kaggle dataset to verify the universality and generality of our model. In addition, we compared our model with three existing methods for solving data imbalance, including downsampling, sliding windows and recombination, in order to evaluate the superiority and effectiveness of DiffEEG.

The main contributions our work makes are as follows:

- We propose a method of using diffusion model to solve the problem of imbalanced data, which is the first work to introduce diffusion model to the seizure prediction field.
- We verify that our diffusion model is superior to the existing data augmentation methods and can be applied to almost any other machine learning classifier to further improve the prediction performance.
- The model based on DiffEEG and Multi-scale CNN achieves the best performance and outperforms most state-of-the-art methods.

The rest of the paper is organized as follows. Section 2 presents the datasets used in this study and our proposed methods. Section 3 describes our experimental results and

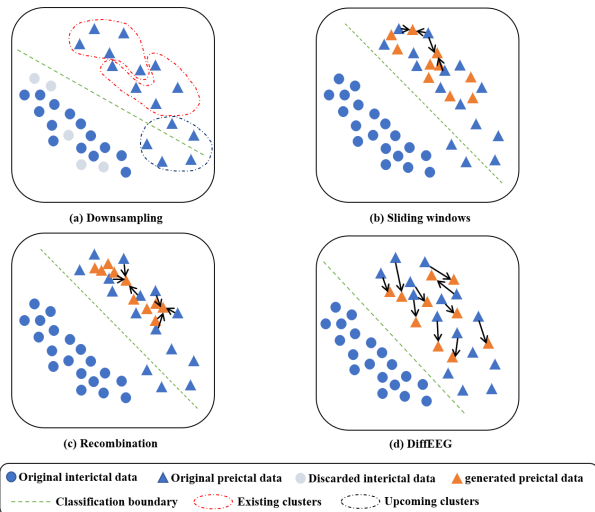


Fig. 1: The distribution illustration of downsampling, sliding windows, recombination and DiffEEG. Each cluster represents the preictal data of a seizure. Distribution from different seizures has similar parts as well as different parts. Downsampling of interictal samples may cause the loss of useful information. When using the sliding windows, the distribution of generated samples is between the front and rear samples. The recombination is implemented within each seizure because samples recombined by segments from different seizures have poor authenticity. Thus, the distribution of recombined samples is limited by the three component samples. Instead, DiffEEG could fully explore the feature space and diffuse the distribution to outward area. The generated samples connect different clusters into a whole.

comparison. Section 4 provides discussion of our methods. Finally, we conclude our work in Section 5.

II. METHODOLOGY

A. Dataset

The CHB-MIT dataset contains scalp EEG (sEEG) data from 23 pediatric patients with 844 h of continuous sEEG recording and 163 seizures. The sEEG signals were captured with use of 22 electrodes at a sampling rate of 256 Hz [43]. To guarantee the consistency of our approach, according to [30], we select 18 channels common to each patient in this study, including FP1-F7, F7-T7, T7-P7, P7-O1, FP1-F3, F3-C3, C3-P3, P3-O1, FP2-F4, F4-C4, C4-P4, P4-O2, FP2-F8, F8-T8, T8-P8, P8-O2, FZ-CZ, and CZ-PZ. We define the preictal period as 30 min before the occurrence of a seizure. The interictal period is defined as being between at least 4 h before seizure onset and 4 h after seizure end [29]. In this dataset, there are cases where multiple seizures occur close to each other. For the seizure prediction task, we are interested in predicting the leading seizures. Therefore for seizures that are less than 15 min from the previous seizure, we consider them as only one seizure and use the onset of the leading seizure as the onset of the combined seizure. Besides, we consider only patients with fewer than 10 seizures per day for the prediction task because it is not very critical to perform the task for patients having a

seizure every 2 h on average [29]. Moreover, we select patients who have more than three seizures and whose interictal-to-preictal ratio was more than 2:1 for having enough data to train the diffusion model as well as having the necessity to generate preictal samples. With these definitions and considerations, there are 13 patients that meet our requirements. The data information is listed in Table I.

TABLE I: Subject information of the CHB-MIT scalp EEG database.

Patient	Interictal times (h)	preictal times (h)	No. of seizures
Chb-01	17	3.5	7
Chb-02	23	1.5	3
Chb-03	22	3	6
Chb-05	14	2.5	5
Chb-09	46.3	2	4
Chb-10	26	3.4	7
Chb-13	14	3	7
Chb-17	10	1.5	3
Chb-18	24	2.5	5
Chb-19	25	1.5	3
Chb-20	20	3.9	8
Chb-21	23.4	2	4
Chb-23	12.9	3.2	7
Total	277.6	33.5	69

The Kaggle dataset contains 48 seizures and more than 700 h of interictal iEEG recordings from five dogs and two patients [44]. For dogs, the electrode channels are 16 for Dog1-Dog4 and 15 for Dog5. And the sampling rate is 400 Hz. For patients, the electrode channels are 15 for patient1 and 24 for patient. The sampling rate is 5 kHz. Because of the high sampling rate, we don't test our method on these two patients. The data information of five dogs is listed in Table II.

TABLE II: Subject information of the Kaggle iEEG database.

Participant	Interictal hours (h)	preictal hours (h)	No. of seizures
Dog1	80	4	4
Dog2	83.3	7	7
Dog3	240	12	12
Dog4	134	14	14
Dog5	75	5	5
Total	612.3	42	42

B. Diffusion Model

Advances in the diffusion model have provided tractable probabilistic parameterization for describing the model, a stable training procedure with sufficient theoretical support, and a unified loss function design with high simplicity [45]. The diffusion model aims to transform the prior data distribution into random noise and revise the transformations step by step to rebuild a brand new sample with the same distribution as the prior. The process that transforms the starting state into the tractable noise through a Markov chain $q(x_t|x_{t-1})$ is the forward/diffusion process. The process that samples the noise gradients step by step into signals as the starting state through

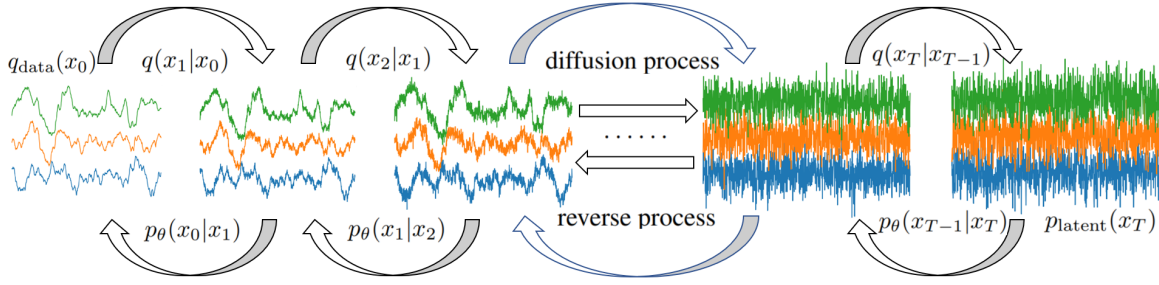


Fig. 2: The diffusion and reverse process in diffusion model.

$p_\theta(x_{t-1}|x_t)$ is called reverse/denoised process. The diffusion and reverse process are showed in Fig. 2.

We define $q_{data}(x_0)$ as the data distribution on $R^{H \times L}$, where H is the EEG channel and L is length of EEG segment. Then we define $x_t \in R^{H \times L}$ for $t = 0, 1, 2, \dots, T$ be a sequence of variables with the same dimension, where t is the index for diffusion steps.

The diffusion process is defined by a fixed Markov chain from data x_0 to the latent variable x_T :

$$q(x_1, \dots, x_T | x_0) = \prod_{i=1}^T q(x_i | x_{i-1}) \quad (1)$$

The whole process gradually converts data x_0 to x_T according to a variance schedule β_1, \dots, β_T .

The reverse process is defined by a Markov chain from x_T to x_0 parameterized by θ :

$$p_{latent}(x_T) = N(0, I) \quad (2)$$

$$p_\theta(x_0, \dots, x_{T-1} | x_T) = \prod_{i=1}^T p_\theta(x_{i-1} | x_i)$$

Given the reverse process, the generative procedure is to first sample an $x_T \sim N(0, I)$, and then sample $x_{t-1} \sim p_\theta(x_{t-1} | x_t)$ for $t = T, T-1, \dots, 1$. The output x_0 is the sampled data. The diffusion model is trained by maximizing its variational lower bound (ELBO):

$$ELBO = E_{q(x_0, \dots, x_T)} \log \frac{p_\theta(x_0, \dots, x_{T-1} | x_T) \times p_{latent}(x_T)}{q(x_1, \dots, x_T | x_0)} \quad (3)$$

Ho et al. has proved that under a certain parameterization, the ELBO of the diffusion model can be calculated in closed-form [37]. Some constants based on the variance schedule $\{\beta_t\}_{t=1}^T$ in the diffusion process are defined as follows:

$$\alpha_t = 1 - \beta_t, \quad \bar{\alpha}_t = \prod_{s=1}^t \alpha_s \quad (4)$$

$$\tilde{\beta}_t = \frac{1 - \bar{\alpha}_{t-1}}{1 - \bar{\alpha}_t} \beta_t \quad \text{for } t > 1 \quad \text{and} \quad \tilde{\beta}_1 = \beta_1$$

We then define the parameterizations of μ_θ and σ_θ :

$$\mu_\theta(x_t, t) = \frac{1}{\sqrt{\alpha_t}} \left(x_t - \frac{\beta_t}{\sqrt{1 - \bar{\alpha}_t}} \varepsilon_\theta(x_t, t) \right) \quad (5)$$

$$\sigma_\theta(x_t, t) = \sqrt{\tilde{\beta}_t}$$

$\varepsilon \sim N(0, I)$, $\varepsilon_\theta : R^{H \times L} \times N \rightarrow R^{H \times L}$ is a neural network taking x_t and the diffusion-step t as inputs. Ho et al. [37] reported that minimizing the following unweighted variant of the ELBO leads to higher generation quality, which is used as the training objective of our model:

$$\min_{\theta} L_{unweighted}(\theta) = E_{x_0, \varepsilon, t} \|\varepsilon - \varepsilon_\theta(\sqrt{\alpha_t} x_0 + \sqrt{1 - \bar{\alpha}_t} \varepsilon, t)\|_2^2 \quad (6)$$

The training and sampling procedures are in Algorithm 1 and 2, respectively.

Algorithm 1 Training

for $i = 1, 2, \dots, N_{iter}$ **do**
 Sample $x_0 \sim q_{data}$, $\varepsilon \sim N(0, I)$, and
 $t \sim \text{Uniform}(1, \dots, T)$
 Take gradient step on
 $\nabla_{\theta} \|\varepsilon - \varepsilon_\theta(\sqrt{\alpha_t} x_0 + \sqrt{1 - \bar{\alpha}_t} \varepsilon, t)\|_2^2$
end for

Algorithm 2 Sampling

Sample $x_T \sim p_{latent} = N(0, I)$
for $t = T, T-1, \dots, 1$ **do**
 Compute $\mu_\theta(x_t, t)$ and $\sigma_\theta(x_t, t)$
 Sample $x_{t-1} \sim p_\theta(x_{t-1} | x_t) =$
 $N(x_{t-1}; \mu_\theta(x_t, t), \sigma_\theta(x_t, t)^2 I)$
end for

C. DiffEEG Architecture

Based on the characteristic of multi-channel EEG signals, we have proposed the diffusion-based network DiffEEG. The network is composed of a stack of N residual layers with residual channels C . These layers are grouped into m blocks and each block has $n = N/m$ layers. We use a bidirectional dilated convolution (Bi-DilConv) with kernel size 3 in each layer. The dilation is doubled at each layer within each block, i.e., $[1, 2, 4, \dots, 2^{n-1}]$. The skip connections from all residual layers are summed before fed into two convolutional layers. A 128-dimensional encoding vector is used for diffusion-step embedding:

$$t_{embedding} = [\sin(10^{\frac{0 \times 4}{63}} t), \dots, \sin(10^{\frac{63 \times 4}{63}} t), \cos(10^{\frac{0 \times 4}{63}} t), \dots, \cos(10^{\frac{63 \times 4}{63}} t)] \quad (7)$$

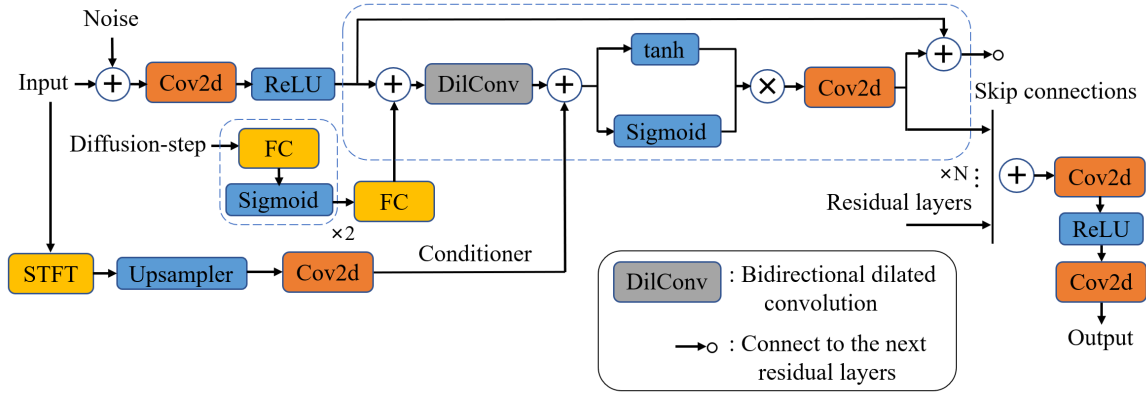


Fig. 3: DiffEEG Architecture.

We divide the EEG signals into 30-s segments as inputs and use the STFT spectrograms of the segments as the conditioner. For CHB-MIT dataset, the window length of STFT is set to 256 with no overlap while for Kaggle dataset the window length is 400 with 300 overlap. We then upsample the STFT spectrogram by applying two layers of transposed 2-D convolution (in time and frequency) to acquire the same shape in time domain as the EEG inputs. After upsampling, we use a layer-specific Conv1×1 to map the frequency domain into 2× residual channels. The conditioner is added as a bias term for the dilated convolution before the gated-tanh nonlinearities in each residual layer. The whole architecture is showed in Fig. 3.

D. Classifier Architecture

We choose three representative SOTA network frameworks as classifiers. They are Spatio-temporal MLP [20], Multi-scale CNN [21] and Transformer [22].

1) *Spatio-temporal MLP*: Spatio-temporal MLP contains two functional blocks: the denoising-weighted block and the MLPs block. The denoising-weighted block consists of a denoising layer, a weighted layer and a reduction layer. The MLPs block consists of an inter-channel layer and an intra-channel layer. Owing to the violent convulsions caused, EEG signals can be easily polluted by ocular artifacts (OAs) and muscle artifacts (MAs) during seizure onset [46]. So there is a denoising layer to remove the artifacts. The weighted layer can automatically learn and assign different weights to each channel and thus strengthen the influence of the most important channels. Apart from that, EEG signals have a large amount of redundant data due to the repetition of specific wave components in spontaneous brain activities. The reduction layer is used to reduce the redundant data so that we can reduce the computational cost and obtain stable results. To extract features of the electrode channels, the MLPs block analyze the spatial dimension: the inter-channel layer applies across different channels to learn inter channel relation, and the intra-channel layer applies independently to each EEG channel to obtain intra channel information. At last, there is an average pooling layer and an FC layer to transform the output of the MLPs block into probability of each seizure state.

2) *Multi-scale CNN*: The framework of Multi-scale CNN consists of two stages: temporal multi-scale stage and spatial multi-scale stage. In the temporal stage, the convolution kernels with larger sizes extract long-term temporal information, while the ones with smaller sizes extract local information. In the spatial stage, by mapping EEG channels to corresponding area of the brain, kernels with larger sizes focus on the information exchange over a large area of brain, while the smaller ones pay attention to the local area. Compared with traditional convolution, the dilated convolution can have a larger receptive field without increasing additional parameters and learn global information more effectively. Therefore, the network uses dilated convolution. An attention-based feature-weighted fusion method is taken to reduce the redundancy and fuse the features. Each feature map obtained by parallel dilated convolution is put into a global average pooling layer followed by the FC layers to learn the weights of feature map. The weighted fused extracted features are finally put into a four-layer CNN classifier.

3) *Transformer*: Transformer is an effective deep learning architecture based on self attention mechanism [47] [48]. we take advantage of the encoder part of the transformer model because the purpose of our task is classification. The Transformer-based model we used mainly consists of three parts: input embedding, positional encoding, and attention module.

- **Input embedding**: The input embedding applies 1D-CNN layer to the raw EEG signals to reduce the input dimension and extract preliminary features.
- **Positional encoding**: The positional encoding is used to extract positional information which is then added to the input embedding [49].
- **Attention module**: The attention module consists of two components: the multi-head attention and the feed-forward network. For the multi-head attention, the query, key, and value vectors (Q, K and V) [47] are generated by multiplying the input by the learned weight matrices W_q , W_k and W_v . The attention values are calculated as below:

$$Attention(Q, K, V) = softmax\left(\frac{QK^T}{\sqrt{d_k}}\right)V \quad (8)$$

where d_k is defined as the embedding dimension. For the feed-forward network, two FC layers is used to extract deeper information by mapping the data to a high-dimensional space first and then back to the low-dimensional space.

E. Training and Testing

In our work, we use the leave-one-out cross-validation strategy. Specifically, if a patient has N seizures, we have N parts of preictal data. So we divide the whole interictal data into N equal parts. For every cross-validation, we take one part from the interictal data followed by one part from the preictal data as the testing set while the rest of the interictal and preictal data serve as the training set. Since preictal samples are far less than interictal samples in the training set, we employ four methods to solve the imbalanced problem:

- Downsampling [26]: Randomly picking samples from the interictal data until we get the same number as the preictal samples.
- Sliding windows [29]: Sliding windows with length W along the time axis at every step S over preictal EEG signals to create samples.
- Recombination [30]: We first divide each preictal samples into three segments, and then randomly pick three segments to recombine new artificial samples.
- Diffusion model: We use the proposed DiffEEG to generate high-quality preictal samples.

While training DiffEEG, the smaller the loss converges to, the higher the generation quality will be. We randomly cut out EEG samples from the training set and send their STFT spectrograms to the trained model as conditioner. In order to raise the diversity of the produced data, besides the randomly selected spectrograms, we also make use of the recombined spectrograms to each generate half of the data. We randomly pick out three preictal samples from the training set, divide the time dimension of their STFT spectrogram into three segments, and randomly choose one sub-spectrogram from each samples for recombination. The spectrogram is then put into the trained DiffEEG to generate EEG signal. After generating enough preictal samples to equal the interictal samples, we mix them randomly and select 25% of later samples in the training set for validation and the rest for training. During the training process, we choose the best model by using early stop to avoid overfitting. The training stops unless the sensitivity and specificity are both the best for five epochs and the best model is then returned. A flow chart of the main process is shown in Fig. 4.

F. Postprocessing

To reduce false alarms, we use the k-of-n method proposed in [29], in which an alarm is set only if at least k predictions among the last n predictions were positive. Experiments showed that $k = 8$ and $n = 10$ are good choices for efficient prediction. In addition, the refractory period is set to 30 mins in this study to prevent continuous alarm for a short time.

III. EXPERIMENTS AND RESULTS

In this section, we evaluate our model on the CHB-MIT and Kaggle database. The details and evaluation metrics of our experiments are presented, followed by the experimental results and comparisons with several state-of-the-art methods.

A. Experiments and Evaluation Metrics

Before the experiments, the seizure prediction horizon (SPH) and the seizure occurrence period (SOP) need to be defined. we follow the definitions of the SOP and SPH proposed by Maiwald et al. [50]. SPH is the period between seizure alarm and the onset of the seizure, and SOP is the period in which seizures are predicted to occur. For a correct prediction, a seizure onset must be within the SOP. Likewise, a false alarm occurs when the prediction system returns a positive result but no seizure occurs during the SOP. In our experiments, for the CHB-MIT database, the SPH and SOP is set to 1 minute and 30 minutes. For the Kaggle database, the SPH and SOP is set to 5 minute and 60 minutes.

For evaluation metrics, we adopt three metrics to evaluate the performance of our framework: sensitivity (Sens), false prediction rate(FPR), area under the curve (AUC). Sens is formulated as the proportion of seizures correctly predicted to the total number of seizures. FPR is formulated as the number of false alarms per hour. AUC is defined as the area under the receiver operating characteristic curve, which is a metric for evaluating the binary classification performance. Assuming that each class has the same prior probability, the random classification method can obtain an AUC of 0.5, while a perfect classifier can reach 1.0.

B. Results and Comparison

To explore the effectiveness and universality of the data augmentation method by DiffEEG, we conduct the contrast experiments which use downsampling, sliding windows, recombination and DiffEEG respectively to solve the problem of imbalanced data. In the meantime, we utilise three representative network frameworks: MLP, CNN, Transformer as classifiers and test the prediction performance on the CHB-MIT and Kaggle database. The performance is shown in Table III ~ Table VIII.

It is clear that our proposed DiffEEG achieves higher Sens, AUC and lower FPR than other methods on all three classifiers. Compared with the sliding windows and recombination methods, our DiffEEG framework improves Sens by an average of 3.33% and 3.23%, reduces FPR by an average of 0.045/h and 0.045/h, improves AUC by an average of 0.059 and 0.040 on the CHB-MIT database, and improves Sens by an average of 7.07% and 7.17%, reduces FPR by an average of 0.039/h and 0.046/h, improves AUC by an average of 0.046 and 0.042 on the Kaggle database. The contrast experiments show that DiffEEG has obvious advantage over the existing methods in solving the problem of imbalanced data. The seizure prediction performance has been improved significantly by the use of our method, proving that the data generated by DiffEEG has high quality and diversity. The model adds noise to EEG samples

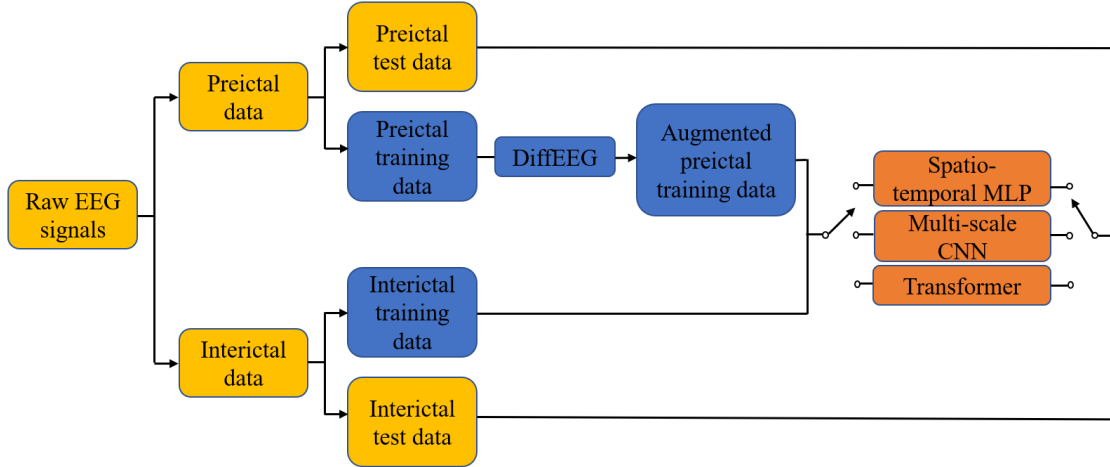


Fig. 4: A flow chart of the proposed method.

TABLE III: Performance of Spatio-temporal MLP on CHB-MIT database.

Patient	Downsampling			Sliding windows			Recombination			DiffEEG		
	Sens (%)	FPR (/h)	AUC	Sens (%)	FPR (/h)	AUC	Sens (%)	FPR (/h)	AUC	Sens (%)	FPR (/h)	AUC
Pat1	100	0	0.9806	100	0	0.9711	100	0	0.9834	100	0	0.9935
Pat2	100	0.043	0.7336	100	0	0.7755	100	0	0.8144	100	0	0.8537
Pat3	83.3	0.091	0.8451	100	0.045	0.8966	100	0.09	0.8611	100	0.045	0.9171
Pat5	100	0.285	0.8380	100	0.071	0.9082	100	0.142	0.8979	100	0	0.9458
Pat9	75	0.216	0.6951	75	0.064	0.6262	75	0.064	0.7101	75	0.043	0.7651
Pat10	71.4	0.269	0.7630	71.4	0.038	0.8190	57.1	0.153	0.7436	85.7	0.038	0.8435
Pat13	100	0.285	0.8903	100	0.285	0.8683	100	0.285	0.8913	100	0.214	0.9086
Pat17	100	0.4	0.8044	100	0.4	0.7883	100	0.3	0.8082	100	0.2	0.8740
Pat18	80	0.083	0.8012	80	0	0.8933	80	0.041	0.8722	80	0	0.9071
Pat19	66.7	0	0.6786	66.7	0	0.8013	66.7	0	0.7950	100	0	0.9488
Pat20	100	0.15	0.9380	100	0.05	0.9542	100	0.05	0.9454	100	0.05	0.9792
Pat21	100	0.427	0.7237	100	0.213	0.7182	100	0.213	0.7683	100	0.213	0.8198
Pat23	100	0	0.9867	100	0	0.9795	100	0	0.9923	100	0	0.9969
Ave	90.5	0.173	0.821	91.8	0.09	0.846	90.7	0.1	0.853	95.4	0.06	0.904

TABLE IV: Performance of Multi-scale CNN on CHB-MIT database.

Patient	Downsampling			Sliding windows			Recombination			DiffEEG		
	Sens (%)	FPR (/h)	AUC	Sens (%)	FPR (/h)	AUC	Sens (%)	FPR (/h)	AUC	Sens (%)	FPR (/h)	AUC
Pat1	100	0	0.9799	100	0	0.9812	100	0	0.9927	100	0	0.9989
Pat2	66.7	0.087	0.6783	100	0	0.6837	66.7	0	0.7462	100	0.044	0.8884
Pat3	100	0.045	0.8735	100	0.045	0.9062	100	0.045	0.9319	100	0	0.9596
Pat5	100	0.214	0.8896	80	0	0.9228	100	0	0.9509	100	0	0.9961
Pat9	75	0.172	0.6552	75	0.064	0.7402	75	0.043	0.7722	75	0	0.8244
Pat10	85.7	0.307	0.7447	85.7	0.115	0.7529	85.7	0.192	0.8098	85.7	0.077	0.8795
Pat13	85.7	0.142	0.8352	85.7	0.5	0.7868	100	0.428	0.8730	100	0.214	0.9469
Pat17	100	0.2	0.8618	100	0.3	0.8804	100	0.3	0.7917	100	0.1	0.8681
Pat18	80	0.083	0.8760	80	0.041	0.8854	80	0	0.8920	80	0	0.8987
Pat19	100	0.2	0.7919	100	0.08	0.9069	100	0	0.9746	100	0	0.9898
Pat20	100	0.3	0.9337	100	0.15	0.9636	100	0.1	0.9723	100	0.05	0.9853
Pat21	100	0.427	0.7548	100	0.256	0.8448	100	0.3	0.9052	100	0.182	0.8967
Pat23	100	0.077	0.9800	100	0.077	0.9890	100	0	0.9923	100	0	0.9872
Ave	91.8	0.173	0.835	92.8	0.125	0.865	92.9	0.108	0.893	95.4	0.05	0.932

TABLE V: Performance of Transformer on CHB-MIT database.

Patient	Downsampling			Sliding windows			Recombination			DiffEEG		
	Sens (%)	FPR (/h)	AUC	Sens (%)	FPR (/h)	AUC	Sens (%)	FPR (/h)	AUC	Sens (%)	FPR (/h)	AUC
Pat1	100	0	0.9861	100	0	0.9899	100	0.059	0.9854	100	0	0.9954
Pat2	100	0.087	0.7642	100	0	0.8321	100	0	0.8205	100	0	0.9096
Pat3	66.7	0.09	0.7776	83.3	0.045	0.8835	100	0.136	0.8873	100	0.045	0.9225
Pat5	100	0.142	0.7840	100	0.071	0.8646	100	0.428	0.8175	100	0.142	0.9344
Pat9	50	0.086	0.6327	75	0.064	0.7738	75	0.108	0.7869	75	0.043	0.8384
Pat10	85.7	0.307	0.7130	85.7	0.192	0.7795	85.7	0.038	0.7833	85.7	0.077	0.8556
Pat13	100	0.285	0.9204	100	0.357	0.9303	100	0.214	0.9353	100	0.214	0.9589
Pat17	100	0.1	0.8946	100	0.1	0.8750	100	0.1	0.9017	100	0.1	0.9421
Pat18	80	0.083	0.7412	80	0.041	0.8069	80	0	0.7849	80	0	0.8331
Pat19	66.7	0.4	0.7739	66.7	0.08	0.7869	66.7	0	0.7857	100	0.04	0.9061
Pat20	100	0.15	0.9435	100	0.1	0.9631	100	0.1	0.9604	100	0.05	0.9828
Pat21	100	0.427	0.7976	100	0.128	0.8654	100	0.085	0.8819	100	0.085	0.9228
Pat23	100	0	0.9808	100	0	0.9910	100	0	0.9916	100	0	0.9941
Ave	88.4	0.166	0.824	91.6	0.091	0.872	92.9	0.097	0.893	95.4	0.06	0.923

TABLE VI: Performance of Spatio-temporal MLP on Kaggle database.

Patient	Downsampling			Sliding windows			Recombination			DiffEEG		
	Sens (%)	FPR (/h)	AUC	Sens (%)	FPR (/h)	AUC	Sens (%)	FPR (/h)	AUC	Sens (%)	FPR (/h)	AUC
Dog1	50	0.262	0.5491	50	0.2	0.5907	50	0.225	0.5638	75	0.25	0.6213
Dog2	100	0.264	0.7866	100	0.228	0.8311	100	0.288	0.8229	100	0.216	0.8607
Dog3	83.3	0.179	0.7196	83.3	0.17	0.7215	83.3	0.158	0.7492	91.7	0.154	0.7855
Dog4	85.7	0.358	0.6632	85.7	0.373	0.6652	92.9	0.38	0.6719	92.9	0.298	0.7136
Dog5	100	0.173	0.8153	100	0.133	0.8313	100	0.133	0.8521	100	0.093	0.8641
Ave	83.8	0.247	0.707	83.8	0.221	0.728	85.2	0.237	0.732	91.9	0.20	0.769

TABLE VII: Performance of Multi-scale CNN on Kaggle database.

Patient	Downsampling			Sliding windows			Recombination			DiffEEG		
	Sens (%)	FPR (/h)	AUC	Sens (%)	FPR (/h)	AUC	Sens (%)	FPR (/h)	AUC	Sens (%)	FPR (/h)	AUC
Dog1	50	0.187	0.6305	50	0.225	0.6177	50	0.2	0.6481	75	0.138	0.69
Dog2	100	0.204	0.8728	100	0.144	0.8865	100	0.132	0.8927	100	0.096	0.9065
Dog3	91.7	0.116	0.7880	91.7	0.138	0.77	83.3	0.1	0.7849	100	0.1	0.83
Dog4	85.7	0.268	0.7188	92.9	0.306	0.7265	92.9	0.239	0.7343	92.9	0.23	0.7686
Dog5	100	0.066	0.8886	100	0.053	0.8716	100	0.053	0.8877	100	0.04	0.9147
Ave	85.5	0.168	0.780	86.9	0.173	0.774	85.2	0.145	0.790	93.6	0.12	0.822

TABLE VIII: Performance of Transformer on Kaggle database.

Patient	Downsampling			Sliding windows			Recombination			DiffEEG		
	Sens (%)	FPR (/h)	AUC	Sens (%)	FPR (/h)	AUC	Sens (%)	FPR (/h)	AUC	Sens (%)	FPR (/h)	AUC
Dog1	50	0.225	0.6013	50	0.15	0.5941	50	0.125	0.5962	75	0.138	0.6387
Dog2	100	0.156	0.8697	100	0.144	0.8972	100	0.168	0.8508	100	0.12	0.9166
Dog3	83.3	0.1	0.7607	91.7	0.104	0.7435	91.7	0.104	0.7644	91.7	0.033	0.8155
Dog4	78.6	0.47	0.6449	78.6	0.3	0.68	78.6	0.447	0.6391	85.7	0.2	0.7243
Dog5	100	0.133	0.8166	100	0.067	0.8478	100	0.08	0.8756	100	0.053	0.9179
Ave	82.4	0.217	0.739	84.1	0.153	0.753	84.1	0.185	0.745	90.5	0.11	0.803

step by step and tries to convert the noisy samples into noise added. During this diffusion process the distribution of EEG data is learned and explored. Thus, the data produced in the denoised process can diffuse the distribution to outward areas and narrow the distance between different clusters. When the data cluster of an upcoming seizure has few nearby distribution with the existing clusters, the seizure will be difficult to predict. The distribution of data generated by sliding windows or recombination is restricted by the original data and cannot be fully explored, so their improvement to prediction performance is limited.

Among the three classification network, Multi-scale CNN wins the best performance. The combination of DiffEEG and Multi-scale CNN achieves an average Sens, FPR, AUC of 95.4%, 0.05/h, 0.932 on the CHB-MIT database and an average Sens, FPR, AUC of 93.6%, 0.12/h, 0.822 on the Kaggle dataset. Although the blocks in Spatio-temporal MLP can extract inter-channel and intra-channel information, the fully connected structure of MLPs determines that the efficiency of data processing is not high. The lack of weight sharing mechanism also leads to the huge amount of parameters, making it difficult to converge to optimal result. So the performance of Spatio-temporal MLP is lower than Multi-scale CNN and Transformer. For Transformer, the input embedding and position encoding can capture the global information of data. The attention module can learn the relation between features and strengthen the role of key information. For Multi-scale CNN, the local perception ability of convolution makes it easier to extract local information. By the use of dilated convolution, spatial and temporal features of different scales can be extracted, providing multi-scale information for seizure prediction. In the meantime, the model also utilizes attention mechanism as Transformer to assign weights to features and focus on the critical representation. Therefore, the Multi-scale CNN network obtains the best effects. MLP, CNN and Transformer are the most representative frameworks in deep learning and almost all classifiers are based on them. As our proposed DiffEEG shows superiority on these three networks, it is proven that DiffEEG can be applied to almost any other classifier to significantly improve the seizure prediction performance.

To further measure our proposed model, we compare the performance of our model with several state-of-the-art methods that used the same CHB-MIT database. The comparison result is shown in Table 9. It can be seen that our method achieves the optimal performance, making it superior to all the other state-of-the-art approaches.

IV. DISCUSSION

Despite decades of development of medical technology, the collection of high-quality EEG data still requires relatively expensive hardware and plenty of participant time [33]. Besides, additional practical challenges related to data collection exist such as headache and surgical infection due to implanted device and accumulation of fluid around implantation area. Data collection procedures are very costly because the medical experts are required in case of emergencies. However, it is the

high-quality EEG data that plays an important role in machine learning classification. So how to generate new samples that have the most benefit to the classifier? Data augmentation is the process that generates new samples to augment a small or imbalanced dataset by transforming existing samples. It holds the promise to increase the accuracy and stability of the classification. Exposing the classifiers to varied training samples makes the model less biased and more robust to transformations [54]. For traditional data augmentation methods such as sliding windows and recombination, although they can increase the quantity of preictal samples, the generated samples have too much repeated information whose distribution is limited by the existing data [31]. In practice, the distribution of EEG signals varies over time due to the changes in external environment and mental states of patients. The epileptic representation in different preictal time varies as well if the location or mode of abnormal discharge is different [32]. Traditional data augmentation methods cannot provide new information for data distribution. Thus, when the upcoming preictal time is difficult to distinguish, their improvement for prediction performance is unsatisfactory. Generative deep learning methods such as GAN and diffusion model can generate synthetic data with new information [55]. Compared with GAN, diffusion models have multiple advantages: in terms of training difficulty, GAN is more difficult to train because the gradients of the generator and discriminator interact with each other during the training process. If the design is unreasonable, the gradients may disappear or explode, leading to unstable sample quality. In contrast, diffusion models have a simple loss function and a stable training process, with a stable decrease in loss during training, greatly reducing the training difficulty and providing more stable and reliable sample quality. In terms of sample diversity, samples generated by GAN are prone to mode collapse, which means that the model may only generate samples similar to a limited number of initial data once trapped in local minimum during training, resulting in a lack of diversity and richness. In contrast, the basic idea of diffusion model is to gradually transform random noise into output signals through a series of sampling. For each diffusion step, the signal value at current point is influenced by the previous and subsequent signal values, thereby better capturing local details. Models with different diffusion steps can be regarded as multiple models with shared weights, which can better explore the data distribution and provide more diversity [42]. Therefore, diffusion models have the best advantage in data augmentation.

The generation of multichannel EEG signals has been a challenge to researchers for a long time. As a result, the existing generative models either choose to generate the feature maps of EEG signals or respectively generate signals of single channel before combining the channels in case that the model cannot fully learn the representations of multichannel EEG signals. Our proposed model, DiffEEG, can overcome the challenge and directly generate signals of the whole channels. The real and synthetic samples generated by DiffEEG of 18 channels and 30-s duration are shown in Fig. 5. To further inspect the details of the samples, we only select the first three channels for 10s as shown in Fig. 6. Visual inspection cannot

TABLE IX: Comparison to existing methods on CHB-MIT database.

Authors	Database	Features	Classifier	No. of seizures	No. of subjects	Sens(%)	FPR(/h)	AUC	Interictal distance(min)	Preictal length(min)
Troung et al. 2018 [29]}	CHB-MIT	STFT	CNN	64	13	81.2	0.16	-	240	30
Ozcan et al. 2019 [18]	CHB-MIT	Spectral power Statistical moments Hjorth parameters	3D CNN	77	16	85.7	0.096	-	240	60
Zhang et al. 2020 [30]	CHB-MIT	Common spatial pattern statistics	CNN	156	23	92	0.12	0.900	30	30
Yang et al. 2021 [51]	CHB-MIT	STFT	RDANet	64	13	89.3	-	0.913	240	30
Li et al. 2022 [52]	CHB-MIT	FB-CapsNet	FB-CapsNet	105	19	93.4	0.096	0.928	240	30
Zhao et al. 2022 [53]	CHB-MIT	raw EEG signals	AddNet-SCL	105	19	93.0	0.094	0.929	240	30
Our work	CHB-MIT	raw EEG signals generated EEG	MLP CNN Transformer	69	13	95.4	0.05	0.932	240	30

evaluate the quality of generated data. Therefore, we carry out seizure prediction experiments to test the contributions of synthetic data. The results verify that the data generated by DiffEEG can greatly improve the prediction performance and beat the existing data augmentation methods in various situations.

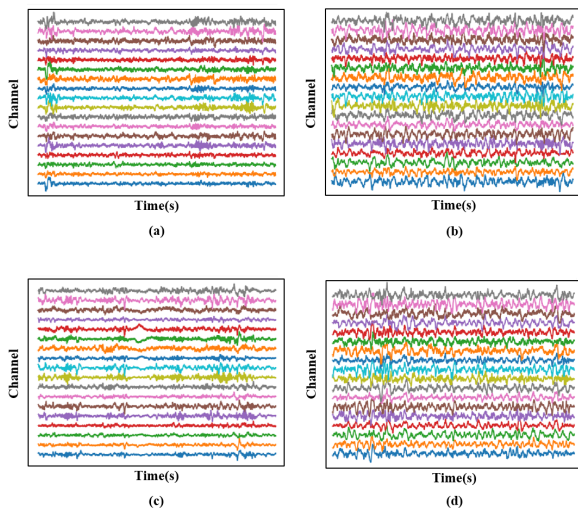


Fig. 5: Real and synthetic samples of 18 channels and 30-s duration. (a)(b) are real samples and (c)(d) are synthetic samples. The amplitudes of all samples are normalized to the same range.

V. CONCLUSION

In this article, we propose a novel and effective data augmentation method by the use of diffusion model. We conduct contrast experiments on our proposed method with three existing methods of solving the problem of imbalanced data: downsampling, sliding windows and recombination. We evaluate the prediction performance on three representative classifiers to verify the effectiveness and generality of DiffEEG. The results prove that the data generated by DiffEEG achieves better performance on all three classification networks. Among them, the model with DiffEEG and Multi-scale CNN has the best performance with an average Sens, FPR, AUC of 95.4%, 0.05/h, 0.932 on the CHB-MIT database and

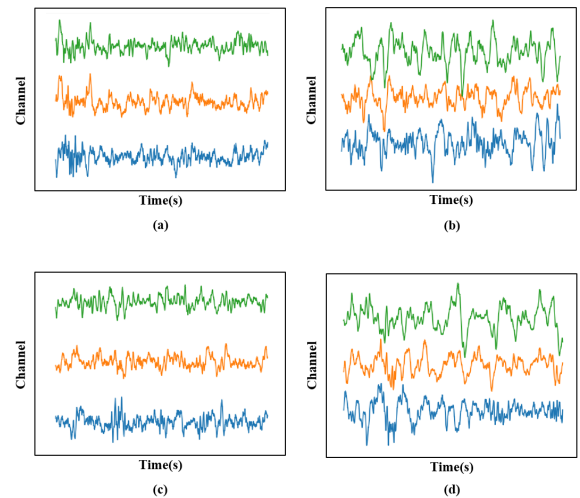


Fig. 6: The enlarged real and synthetic signals of 3 channels and 10-s duration. (a)(b) are from real samples and (c)(d) are from synthetic samples. The amplitudes of all samples are normalized to the same range.

an average Sens, FPR, AUC of 93.6%, 0.12/h, 0.822 on the Kaggle database, both reaching the state-of-the-art level. To the best of our knowledge, our work is the first diffusion model used in epileptic EEG generation, creating a new and effective way to solve the imbalanced data. This model can be widely applied to all kinds of seizure prediction classifiers to improve the classification performance significantly.

REFERENCES

- [1] R. S. Fisher, C. Acevedo, A. Arzimanoglou, A. Bogacz, J. H. Cross, C. E. Elger, J. Engel Jr, L. Forsgren, J. A. French, M. Glynn *et al.*, "Ilae official report: a practical clinical definition of epilepsy," *Epilepsia*, vol. 55, no. 4, pp. 475–482, 2014.
- [2] W. H. Organization *et al.*, *Epilepsy: a public health imperative*. World Health Organization, 2019.
- [3] B. Maimaiti, H. Meng, Y. Lv, J. Qiu, Z. Zhu, Y. Xie, Y. Li, W. Zhao, J. Liu, M. Li *et al.*, "An overview of eeg-based machine learning methods in seizure prediction and opportunities for neurologists in this field," *Neuroscience*, vol. 481, pp. 197–218, 2022.
- [4] D. Jacobs, Y. H. Liu, T. Hilton, M. Del Campo, P. L. Carlen, and B. L. Bardakjian, "Classification of scalp eeg states prior to clinical seizure onset," *IEEE journal of translational engineering in health and medicine*, vol. 7, pp. 1–3, 2019.

- [5] L. Xiao, C. Li, Y. Wang, J. Chen, W. Si, C. Yao, X. Li, C. Duan, and P.-A. Heng, "Automatic localization of seizure onset zone from high-frequency seeg signals: A preliminary study," *IEEE Journal of Translational Engineering in Health and Medicine*, vol. 9, pp. 1–10, 2021.
- [6] B. Direito, C. A. Teixeira, F. Sales, M. Castelo-Branco, and A. Dourado, "A realistic seizure prediction study based on multiclass svm," *International journal of neural systems*, vol. 27, no. 03, p. 1750006, 2017.
- [7] L. Kuhlmann, K. Lehnertz, M. P. Richardson, B. Schelter, and H. P. Zaveri, "Seizure prediction—ready for a new era," *Nature Reviews Neurology*, vol. 14, no. 10, pp. 618–630, 2018.
- [8] H. Daoud and M. A. Bayoumi, "Efficient epileptic seizure prediction based on deep learning," *IEEE transactions on biomedical circuits and systems*, vol. 13, no. 5, pp. 804–813, 2019.
- [9] L. D. Iasemidis, J. Chris Sackellares, H. P. Zaveri, and W. J. Williams, "Phase space topography and the lyapunov exponent of electrocorticograms in partial seizures," *Brain topography*, vol. 2, pp. 187–201, 1990.
- [10] M. Le Van Quyen, J. Martinerie, M. Baulac, and F. Varela, "Anticipating epileptic seizures in real time by a non-linear analysis of similarity between eeg recordings," *Neuroreport*, vol. 10, no. 10, pp. 2149–2155, 1999.
- [11] M. Bandarabadi, C. A. Teixeira, J. Rasekhi, and A. Dourado, "Epileptic seizure prediction using relative spectral power features," *Clinical Neurophysiology*, vol. 126, no. 2, pp. 237–248, 2015.
- [12] J. Birjandtalab, M. B. Pouyan, D. Cogan, M. Nourani, and J. Harvey, "Automated seizure detection using limited-channel eeg and non-linear dimension reduction," *Computers in biology and medicine*, vol. 82, pp. 49–58, 2017.
- [13] A. Subasi, J. Kevric, and M. Abdullah Canbaz, "Epileptic seizure detection using hybrid machine learning methods," *Neural Computing and Applications*, vol. 31, pp. 317–325, 2019.
- [14] X. Chen, C. Li, A. Liu, M. J. McKeown, R. Qian, and Z. J. Wang, "Toward open-world electroencephalogram decoding via deep learning: A comprehensive survey," *IEEE Signal Processing Magazine*, vol. 39, no. 2, pp. 117–134, 2022.
- [15] L. Chisci, A. Mavino, G. Perferi, M. Sciandrone, C. Anile, G. Colicchio, and F. Fuggetta, "Real-time epileptic seizure prediction using ar models and support vector machines," *IEEE Transactions on Biomedical Engineering*, vol. 57, no. 5, pp. 1124–1132, 2010.
- [16] L. Kuhlmann, P. Karoly, D. R. Freestone, B. H. Brinkmann, A. Temko, A. Barachant, F. Li, G. Titericz Jr, B. W. Lang, D. Lavery *et al.*, "Epilepsyecosystem.org: crowd-sourcing reproducible seizure prediction with long-term human intracranial eeg," *Brain*, vol. 141, no. 9, pp. 2619–2630, 2018.
- [17] D. Liang, A. Liu, Y. Gao, C. Li, R. Qian, and X. Chen, "Semi-supervised domain-adaptive seizure prediction via feature alignment and consistency regularization," *IEEE Transactions on Instrumentation and Measurement*, vol. 72, pp. 1–12, 2023.
- [18] A. R. Ozcan and S. Erturk, "Seizure prediction in scalp eeg using 3d convolutional neural networks with an image-based approach," *IEEE Transactions on Neural Systems and Rehabilitation Engineering*, vol. 27, no. 11, pp. 2284–2293, 2019.
- [19] B. Sun, J.-J. Lv, L.-G. Rui, Y.-X. Yang, Y.-G. Chen, C. Ma, and Z.-K. Gao, "Seizure prediction in scalp eeg based channel attention dual-input convolutional neural network," *Physica A: Statistical Mechanics and its Applications*, vol. 584, p. 126376, 2021.
- [20] C. Li, C. Shao, R. Song, G. Xu, X. Liu, R. Qian, and X. Chen, "Spatio-temporal mlp network for seizure prediction using eeg signals," *Measurement*, vol. 206, p. 112278, 2023.
- [21] Y. Gao, X. Chen, A. Liu, D. Liang, L. Wu, R. Qian, H. Xie, and Y. Zhang, "Pediatric seizure prediction in scalp eeg using a multi-scale neural network with dilated convolutions," *IEEE journal of translational engineering in health and medicine*, vol. 10, pp. 1–9, 2022.
- [22] Y. Gao, A. Liu, X. Cui, R. Qian, and X. Chen, "A general sample-weighted framework for epileptic seizure prediction," *Computers in Biology and Medicine*, vol. 150, p. 106169, 2022.
- [23] M. J. Cook, T. J. O'Brien, S. F. Berkovic, M. Murphy, A. Morokoff, G. Fabinyi, W. D'Souza, R. Yerra, J. Archer, L. Litewka *et al.*, "Prediction of seizure likelihood with a long-term, implanted seizure advisory system in patients with drug-resistant epilepsy: a first-in-man study," *The Lancet Neurology*, vol. 12, no. 6, pp. 563–571, 2013.
- [24] M. Ihle, H. Feldwisch-Drentrup, C. A. Teixeira, A. Witon, B. Schelter, J. Timmer, and A. Schulze-Bonhage, "Epilepsiae—a european epilepsy database," *Computer methods and programs in biomedicine*, vol. 106, no. 3, pp. 127–138, 2012.
- [25] P. Branco, L. Torgo, and R. P. Ribeiro, "A survey of predictive modeling on imbalanced domains," *ACM computing surveys (CSUR)*, vol. 49, no. 2, pp. 1–50, 2016.
- [26] H. Khan, L. Marcuse, M. Fields, K. Swann, and B. Yener, "Focal onset seizure prediction using convolutional networks," *IEEE Transactions on Biomedical Engineering*, vol. 65, no. 9, pp. 2109–2118, 2017.
- [27] J. Mathew, M. Luo, C. K. Pang, and H. L. Chan, "Kernel-based smote for svm classification of imbalanced datasets," in *IECON 2015-41st Annual Conference of the IEEE Industrial Electronics Society*. IEEE, 2015, pp. 001 127–001 132.
- [28] Y. Cui, F. Zhou, Y. Lin, and S. Belongie, "Fine-grained categorization and dataset bootstrapping using deep metric learning with humans in the loop," in *Proceedings of the IEEE conference on computer vision and pattern recognition*, 2016, pp. 1153–1162.
- [29] N. D. Truong, A. D. Nguyen, L. Kuhlmann, M. R. Bonyadi, J. Yang, S. Ippolito, and O. Kavehei, "Convolutional neural networks for seizure prediction using intracranial and scalp electroencephalogram," *Neural Networks*, vol. 105, pp. 104–111, 2018.
- [30] Y. Zhang, Y. Guo, P. Yang, W. Chen, and B. Lo, "Epilepsy seizure prediction on eeg using common spatial pattern and convolutional neural network," *IEEE Journal of Biomedical and Health Informatics*, vol. 24, no. 2, pp. 465–474, 2019.
- [31] A. Antoniou, A. Storkey, and H. Edwards, "Data augmentation generative adversarial networks," *arXiv preprint arXiv:1711.04340*, 2017.
- [32] Y. Qi, L. Ding, Y. Wang, and G. Pan, "Learning robust features from nonstationary brain signals by multiscale domain adaptation networks for seizure prediction," *IEEE Transactions on Cognitive and Developmental Systems*, vol. 14, no. 3, pp. 1208–1216, 2021.
- [33] K. Rasheed, J. Qadir, T. J. O'Brien, L. Kuhlmann, and A. Razi, "A generative model to synthesize eeg data for epileptic seizure prediction," *IEEE Transactions on Neural Systems and Rehabilitation Engineering*, vol. 29, pp. 2322–2332, 2021.
- [34] T. Salimans, I. Goodfellow, W. Zaremba, V. Cheung, A. Radford, and X. Chen, "Improved techniques for training gans," *Advances in neural information processing systems*, vol. 29, 2016.
- [35] G. Giannone, D. Nielsen, and O. Winther, "Few-shot diffusion models," *arXiv preprint arXiv:2205.15463*, 2022.
- [36] Z. Kong, W. Ping, J. Huang, K. Zhao, and B. Catanzaro, "Dif-fwave: A versatile diffusion model for audio synthesis," *arXiv preprint arXiv:2009.09761*, 2020.
- [37] J. Ho, A. Jain, and P. Abbeel, "Denoising diffusion probabilistic models," *Advances in Neural Information Processing Systems*, vol. 33, pp. 6840–6851, 2020.
- [38] A. Kebaili, J. Lapuyade-Lahorgue, and S. Ruan, "Deep learning approaches for data augmentation in medical imaging: A review," *Journal of Imaging*, vol. 9, no. 4, p. 81, 2023.
- [39] W. H. Pinaya, P.-D. Tudosiu, J. Dafflon, P. F. Da Costa, V. Fernandez, P. Nachev, S. Ourselin, and M. J. Cardoso, "Brain imaging generation with latent diffusion models," in *Deep Generative Models: Second MICCAI Workshop, DGM4MICCAI 2022, Held in Conjunction with MICCAI 2022, Singapore, September 22, 2022, Proceedings*. Springer, 2022, pp. 117–126.
- [40] H. Chung, E. S. Lee, and J. C. Ye, "Mr image denoising and super-resolution using regularized reverse diffusion," *IEEE Transactions on Medical Imaging*, 2022.
- [41] P. Chambon, C. Bluethgen, J.-B. Delbrouck, R. Van der Sluijs, M. Polacin, J. M. Z. Chaves, T. M. Abraham, S. Purohit, C. P. Langlotz, and A. Chaudhari, "Roentgen: Vision-language foundation model for chest x-ray generation," *arXiv preprint arXiv:2211.12737*, 2022.
- [42] P. Dhariwal and A. Nichol, "Diffusion models beat gans on image synthesis," *Advances in Neural Information Processing Systems*, vol. 34, pp. 8780–8794, 2021.
- [43] A. H. Shoeb, "Application of machine learning to epileptic seizure onset detection and treatment," Ph.D. dissertation, Massachusetts Institute of Technology, 2009.
- [44] B. H. Brinkmann, J. Wagenaar, D. Abbot, P. Adkins, S. C. Bosshard, M. Chen, Q. M. Tieng, J. He, F. Muñoz-Almaraz, P. Botella-Rocamora *et al.*, "Crowdsourcing reproducible seizure forecasting in human and canine epilepsy," *Brain*, vol. 139, no. 6, pp. 1713–1722, 2016.
- [45] H. Cao, C. Tan, Z. Gao, G. Chen, P.-A. Heng, and S. Z. Li, "A survey on generative diffusion model," *arXiv preprint arXiv:2209.02646*, 2022.
- [46] J. Hu, C.-s. Wang, M. Wu, Y.-x. Du, Y. He, and J. She, "Removal of eeg and emg artifacts from eeg using combination of functional link neural network and adaptive neural fuzzy inference system," *Neurocomputing*, vol. 151, pp. 278–287, 2015.

- [47] A. Vaswani, N. Shazeer, N. Parmar, J. Uszkoreit, L. Jones, A. N. Gomez, Ł. Kaiser, and I. Polosukhin, "Attention is all you need," *Advances in neural information processing systems*, vol. 30, 2017.
- [48] Z. Liu, Y. Lin, Y. Cao, H. Hu, Y. Wei, Z. Zhang, S. Lin, and B. Guo, "Swin transformer: Hierarchical vision transformer using shifted windows," in *Proceedings of the IEEE/CVF international conference on computer vision*, 2021, pp. 10 012–10 022.
- [49] J. Lee and K. Toutanova, "Pre-training of deep bidirectional transformers for language understanding," *arXiv preprint arXiv:1810.04805*, 2018.
- [50] T. Maiwald, M. Winterhalder, R. Aschenbrenner-Scheibe, H. U. Voss, A. Schulze-Bonhage, and J. Timmer, "Comparison of three nonlinear seizure prediction methods by means of the seizure prediction characteristic," *Physica D: nonlinear phenomena*, vol. 194, no. 3-4, pp. 357–368, 2004.
- [51] X. Yang, J. Zhao, Q. Sun, J. Lu, and X. Ma, "An effective dual self-attention residual network for seizure prediction," *IEEE Transactions on Neural Systems and Rehabilitation Engineering*, vol. 29, pp. 1604–1613, 2021.
- [52] C. Li, Y. Zhao, R. Song, X. Liu, R. Qian, and X. Chen, "Patient-specific seizure prediction from electroencephalogram signal via multi-channel feedback capsule network," *IEEE Transactions on Cognitive and Developmental Systems*, 2022.
- [53] Y. Zhao, C. Li, X. Liu, R. Qian, R. Song, and X. Chen, "Patient-specific seizure prediction via adder network and supervised contrastive learning," *IEEE Transactions on Neural Systems and Rehabilitation Engineering*, vol. 30, pp. 1536–1547, 2022.
- [54] E. Lashgari, D. Liang, and U. Maoz, "Data augmentation for deep-learning-based electroencephalography," *Journal of Neuroscience Methods*, vol. 346, p. 108885, 2020.
- [55] B. Trabucco, K. Doherty, M. Gurinas, and R. Salakhutdinov, "Effective data augmentation with diffusion models," *arXiv preprint arXiv:2302.07944*, 2023.